Applied Surface Science 257 (2011) 1813–1823

Contents lists available at ScienceDirect

Applied Surface Science

journal homepage: www.elsevier.com/locate/apsusc

Surface bioactivity modification of titanium by CO_2 plasma treatment and induction of hydroxyapatite: In vitro and in vivo studies

Xixue Hu[a,d], Hong Shen[b], Kegang Shuai[a], Enwei Zhang[a,d], Yanjie Bai[a], Yan Cheng[a], Xiaoling Xiong[a], Shenguo Wang[b], Jing Fang[a,d,*], Shicheng Wei[a,c,**]

[a] Center for Biomedical Materials and Tissue Engineering, Academy for Advanced Interdisciplinary Studies, Peking University, Beijing 100871, China
[b] BNLMS, State Key Laboratory of Polymer Physics & Chemistry, Institute of Chemistry, Chinese Academy of Sciences, Beijing 100190, China
[c] Department of Oral and Maxillofacial Surgery, School of Stomatology, Peking University, Beijing 100081, China
[d] College of Engineering, Peking University, Beijing 100871, China

ARTICLE INFO

Article history:
Received 12 March 2010
Received in revised form 13 June 2010
Accepted 22 August 2010
Available online 17 October 2010

Keywords:
Titanium
Surface modification
Carbon dioxide plasma
Hydroxyapatite
Bioactivity

ABSTRACT

Since metallic biomaterials used for orthopedic and dental implants possess a paucity of reactive functional groups, bioactivity modification of these materials is challenging. In the present work, the titanium discs and rods were treated with carbon dioxide plasma and then incubated in a modified simulated body fluid 1.5SBF to obtain a hydroxyapatite layer. Surface hydrophilicity of samples, changes of surface chemistry, surface morphologies of samples, and structural analysis of formed hydroxyapatite were investigated by contact angle to water, X-ray photoelectron spectrometer (XPS), scanning electron microscopy (SEM), Fourier transform infrared (FTIR) and X-ray diffraction (XRD). The results demonstrated that hydrophilicity of titanium surface was improved and hydroxyl groups increased after modification with carbon dioxide plasma treatment. The hydroxyl groups on the surface of titanium were the richest after carbon dioxide plasma treatment under the condition of 20 W for less than 30 s. The hydroxyapatite formability of titanium surface was enhanced by carbon dioxide plasma pretreatment, which was attributed to the surface chemistry. MC3T3-E1 cell as a model cell was cultured on the Ti, CPT-Ti and CPT/SBF-Ti discs in vitro, and the results of the morphology and differentiation of the cell showed that CPT/SBF-Ti was the highest bioactive. The relative parameters of the new bone around the Ti and CPT/SBF-Ti rods including bone mineral density (BMD), a ratio of bone volume to total volume (BV/TV), trabecular thickness (Tb.Th.) and trabecular number (Tb.N.) were analyzed by a micro-computed tomography (micro-CT) after 4-, 8- and 12-week implantation periods in vivo. The results indicated that the CPT/SBF-Ti was more advantageous for new bone formation.

1. Introduction

Titanium is being widely used in various areas of medicine, including artificial joints, orthopedic, dental implants and cardiac stents [1], because of its favorable properties such as good ductility, tensile and fatigue strength, modulus of elasticity matching that of bones, lower allergenicity and excellent resistance to corrosion [2] compared with other metals. However, due to the non-bioactivity, it cannot bond with bone directly and promote new bone formation on its surface at the early stage after implantation. So early implant failure of titanium based materials may occur and some problems during healing may arise especially for patient groups with the diseases such as diabetes, osteoporosis, and chronic inflammation [3–5].

It is widely accepted that the successful implantation for titanium implants is demonstrating excellent osteointegration at the bone–implant interface [1,6]. In order to improve osteointegration, new challenges are to be faced to improve the formation of new bone in direct contact with them at early post-implantation periods [7], to reduce interfacial fibrous tissue formation [8], and to accelerate initial healing times during osteointegration processes even in patients with pathologic bone [9]. Recently, a significant number of methods for surface modification of titanium implants have been proposed, which mainly included two approaches. One approach is based on the control of surface topography with physical and/or chemical change of titanium such as sandblasting, acid-etching, alkaline-heat treatment, and sandblasting and acid-etching [10–12]. Gotfredsen's research [13] demonstrated that a

* Corresponding author at: Department of Oral and Maxillofacial Surgery, School of Stomatology, Peking University, Beijing 100081, China. Tel.: +86 10 62754241; fax: +86 10 62754241.
** Corresponding author at: Center for Biomedical Materials and Tissue Engineering, Academy for Advanced Interdisciplinary Studies, Peking University, Beijing 100871, China. Tel.: +86 10 62753404; fax: +86 10 62753404.
E-mail addresses: jfang@pku.edu.cn (J. Fang), sc-wei@pku.edu.cn (S. Wei).

0169-4332/$ – see front matter © 2010 Published by Elsevier B.V.
doi:10.1016/j.apsusc.2010.08.082

Table 1
Comparison of concentrations (mM) of various ions in human blood plasma, 1.0SBF, 1.5SBF-1 and 1.5SBF-2.

	Na^+	K^+	Ca^{2+}	Mg^{2+}	HCO_3^-	Cl^-	HPO_4^{2-}	SO_4^{2-}
Blood plasma	142.0	5.0	2.5	1.5	27.0	103.0	1.0	0.5
1.0SBF	142.0	5.0	2.5	1.5	4.2	148.0	1.0	0.5
1.5SBF-1	213.1	7.5	3.8	2.3	6.3	221.9	1.5	0.8
1.5SBF-2	213.1	7.5	5.2	2.3	6.3	224.7	1.5	0.8

micro-scale rough surface prepared by grit blasting and subsequent acid-etching was capable of rapid and increased bone accrual and Buser's preliminary results [14] suggested that SLA modified implants could further reduce the healing time to 3–4 weeks. Kokubo et al. [15] and Kim et al. [16] reported that NaOH-treated titanium had good bone conductivity. The other approach is immobilization of bioactive molecules on the implant surface such as hyalurone [17], collage [18,19], BMP [20], and calcium phosphate [21,22] by physicochemical and biochemical methods.

Hydroxyapatite (HA) exhibits excellent biocompatibility and stimulates formation of new bone because of its chemical and structural similarities to bone and tooth minerals. So HA is widely used in bone reconstruction [23–25]. HA coating on the titanium surface had been obtained by plasma spraying [26], induction in simulated body fluid [27] and so on. Hanawa et al. [21] found that calcium ion implantation improved the ability of titanium to induce the formation of calcium phosphate precipitates and their experiments in vivo demonstrated that calcium ion-implanted titanium was superior to unimplanted titanium from the perspective of bone conduction.

However, the coated apatite is easily removed from the metal surface because there is no interaction between the substrate and the apatite coating obtained by a simple apatite precipitation, and so the application of an apatite precipitation is restricted [28]. Although there are strong interaction between plasma-sprayed hydroxyapatite (HA) coating and titanium, it has characteristics in physiological environments different from bulk HA ceramics because the HA starting particles are completely melted and then rapidly solidified upon impinging the cool substrate during the plasma-spraying process. In order to improve the bonding strength between HA coating and metal substrate, negative functional groups have been introduced onto the surface of metal substrate, and then react with calcium and phosphate to prepare HA coating.

It is well known that plasma treatment and then immobilizing bioactive molecules is a convenient method for modifying the surface of polymer materials [29]. Different groups and chains can be introduced onto the surface of materials by using different gases [30–32]. The previous research showed that appropriate oxygen plasma treatment could not only incorporate –C–O– groups onto the PLGA surface and increase its negative charges, but also produce peaks and valleys on its surface through etching effect [33], which enhanced the bone-like apatite formability of PLGA(70/30) [34]. Shen et al. [35] also reported carbon dioxide plasma treatment can introduce rich oxygen-containing functional groups, such as >C═O, –COOH or –C–O–, onto the surface of the polylactone-type polymers.

Recently, a few of researches on modification of metal surface by plasma have been reported. Thermal deformation of the materials can also be minimized as it is nominally a low-temperature treatment process and sample cooling can be easily implemented [36]. Oxygen plasma implantation into titanium has been conducted to fabricate titanium oxide in order to modify the biocompatibility of titanium and improve the related properties of it [37,38]. Loinza et al. [39] reported that the surface hardness increased by 100% and wear resistance also improved significantly after the treatment. Xie et al. demonstrated titanium surface became rougher and Ti–OH was introduced after sequential water and hydrogen implantation [40]. But it could be seen from the report that its etching effect was far from meeting the demand of implant surface topography for osteointegration.

It is well known from previous reports [41] that several negative oxygen-containing functional groups, including carboxylic acid, hydroxyl, and ketone/aldehyde groups, can be introduced onto the surface of polymers by CO_2 plasma treatment. What's more, negative groups on the chemically treated surface of titanium implant can bond with Ca^{2+} ion in the body fluid and then Ca^{2+} ion reacts with PO_4^{3+} and OH^- to form amorphous calcium phosphate which gradually transformed to bone-like apatite [42,43]. Moreover, surface micro- and nano-structured topography may increase the number of hydroxyapatite nucleation site. In order to research the effect of carbon dioxide plasma treatment on HA formation on titanium substrate, in the present study sandblasted–acid etched titanium was modified by carbon dioxide plasma for the first time, then incubated in 1.5 times modified SBF. It was investigated that the effect of modified titanium on cell growth and differentiation in vitro and the formation of new bone in vivo.

Table 2
Purity and amount of various reagents for preparing 1000 ml of 1.5SBF-1 and 1.5SBF-2 solution.

Reagents	Purity (%)	Amounts	
		1.5SBF-1	1.5SBF-2
NaCl	>99.5	12.054 g	12.054 g
$NaHCO_3$	>99.5	0.528 g	0.528 g
KCl	>99.5	0.338 g	0.338 g
$K_2HPO_4{\cdot}3H_2O$	>99.0	0.345 g	0.345 g
$MgCl_2{\cdot}6H_2O$	>98.0	0.467 g	0.467 g
1.0 M HCl	–	0.8 ml	0.8 ml
$CaCl_2$	>96.0	0.440 g	0.600 g
Na_2SO_4	>99.0	0.108 g	0.108 g
1.0 M NaOH	–	Trace	Trace

2. Materials and methods

2.1. Materials

In this study, a commercially available pure titanium rod, 15 mm in diameter, was used. The titanium rod was cut into discs with a thickness of 1.5 mm and cylinder with the diameter of 3.0 mm and the length of 5.0 mm. The surface of samples was polished in turn with emery paper of 60, 400, 800 and 1200 grit, and washed in an ultrasonic bath for 15 min using acetone, ethanol and distilled water, respectively, then dried at room temperature for 24 h. The above polished rods and discs were sandblasted with large grit of 0.25–0.38 mm and subsequently etched with the mixed acid containing 5.80 mol/L HCl and 8.96 mol/L H_2SO_4 for 30 min at 60 °C, followed by washing as the cleaning process of the polished samples. The obtained samples were kept in vacuum for use.

2.2. Plasma treatment of titanium discs and rods

Plasma treatment was carried out on Samco Plasma Deposition (Model PD-2, 13.56 MHz) under carbon dioxide atmosphere. Titanium discs and rods were placed on the electrode in the plasma

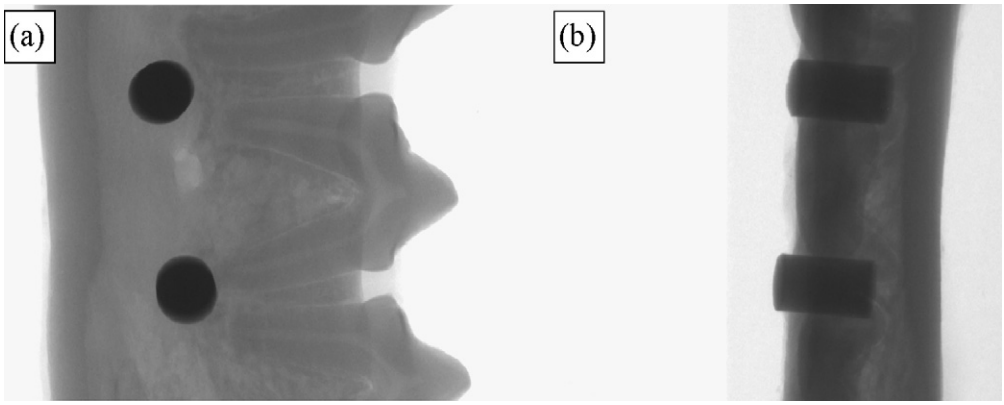

Fig. 1. Observation of the titanium rods inserted in the mandible of a beagle dog by micro-CT. (a) The front view; (b) the side view.

chamber. The chamber was evacuated to less than 10 Pa before filling with carbon dioxide gas. After gaseous pressure of the chamber was stabilized to 20 Pa, glow discharge plasma was created by controlling electrical power at 20 W and radio frequency of 13.56 MHz for a predetermined time. Finally, the plasma-treated sample was further exposed to carbon dioxide atmosphere for another 10 min before the sample was taken out from the chamber.

2.3. Preparation of 1.5SBF incubation solution

In the present study, 1.5SBF was used as an incubation solution for hydroxyapatite formation on the surface of titanium discs and rods. Compared with 1.0SBF (the conventional SBF), the 1.5SBF has ionic concentrations 1.5 times to those of 1.0SBF (Table 1). The reagents and their purity and amounts for preparing 1000 ml of 1.5SBF solution are listed in Table 2. Noticeably, before the addition of $CaCl_2$, a certain amount of HCl was needed to control the solution pH under a lower value (<7.00) to prevent hydroxyapatite precipitation in the solution. 1.5SBF-1 and 1.5SBF-2 were adjusted to a final pH of 7.20 at 36.5 °C with HCl and NaOH. The obtained incubation solution was used immediately to deposit hydroxyapatite onto titanium samples.

2.4. Induction of hydroxyapatite

The untreated or carbon dioxide plasma-treated titanium samples were kept in polypropylene tubes (one per tube) containing 35 ml of incubation solution that was renewed every 3 days. After incubation for 3, 7 and 14 days at 36.5 °C, respectively, the samples were taken out and rinsed with distilled water and dried under vacuum for characterization.

2.5. Surface characterization

Contact angles to water of the treated and untreated titanium discs were measured on air surface of the discs at room temperature using a FACE CA-D type contact angle meter (Kyowa Kaimenkagaku Co. Ltd.). The measuring time for every datum was within 10 s, and 10 data were averaged.

Surface chemical compositions of the samples were investigated by X-ray photoelectron spectrometer (XPS) (Axis Ultra, Japan), and concentrations of various O1s peaks were calculated from the relative O1s peak area.

The surface morphologies of the samples were observed by scanning electron microscopy (SEM, Strata DB235 FIB, Japan) with a voltage of 15 kV, and for elemental analysis by X-ray energy-dispersive spectroscopy (EDS, Genesis, EDAX Inc.).

A few micrograms of the Ca/P precipitate formed on the surface of the sandblasted–acid etched titanium disc incubated in 1.5SBF-2 was scraped off. Then it was mixed with KBr and pressed into plates for structural analysis using Fourier Transform Infrared Spectrometer (Raman950/Magna-IR750, USA). At the same time, the structure of the formed hydroxyapatite on the surface of the titanium disc was also characterized by X-ray diffraction (XRD) using X'Pert diffractometer with Cu Kα radiation (λ = 0.1541 nm) at room temperature. The two θ range was 15–80° at a scanning rate of 8.0°/min.

Table 3
Fraction of oxygen functional groups from high-resolution O1s XPS peaks of titanium disc surface before and after carbon dioxide plasma treatment.

Carbon dioxide plasma treatment	532.7 eV basic OH (%)	531.4 eV acidic OH (%)	530.2 eV O–Ti (%)
None	0	16.64	83.36
20 W, 10 s	9.20	30.75	60.05
20 W, 30 s	8.29	31.57	60.14
20 W, 90 s	6.48	30.18	63.34
20 W, 300 s	6.10	29.86	64.04

2.6. Cell culture

MC3T3-E1 preosteoblasts (ATCC, CRL-2593) were incubated in a carbon dioxide incubator supplied with 5% CO_2 at 37 °C. The culture medium was Alpha Minimum Essential Medium (α-MEM; GIBCO BRL, Carlsbad, CA, USA) supplemented with 10% fetal bovine serum (FBS; MDgenics Inc., USA) and 100 U/cm^3 each of penicillin and streptomycin. When the cells had grown to confluence, they were detached by trypsin/EDTA (0.25% (w/v) trypsin/0.02% (w/v) EDTA) and resuspended in fresh culture medium to the correct concentration for seeding onto various titanium discs.

2.7. Observation of cell morphology

Various titanium discs with a diameter of 15 mm were placed in a 24-well culture plate and MC3T3-E1 cell suspension containing 40,000 cells was poured into each well. After 4 h of incubation, the samples were washed with PBS and fixed with 2.5% glutaraldehyde for 24 h at 4 °C. Then the samples were dehydrated through a series of graded alcohols, free-dried and sputter-coated with gold. Finally the cell morphology was observed by SEM (JSM-6700F, Japan).

2.8. Alkaline phosphatase activity assay

MC3T3-E1 cell suspension containing 40,000 cells was seeded on various titanium discs with a diameter of 15 mm, which were placed in a 24-well culture plate. After 1 day of incubation, the

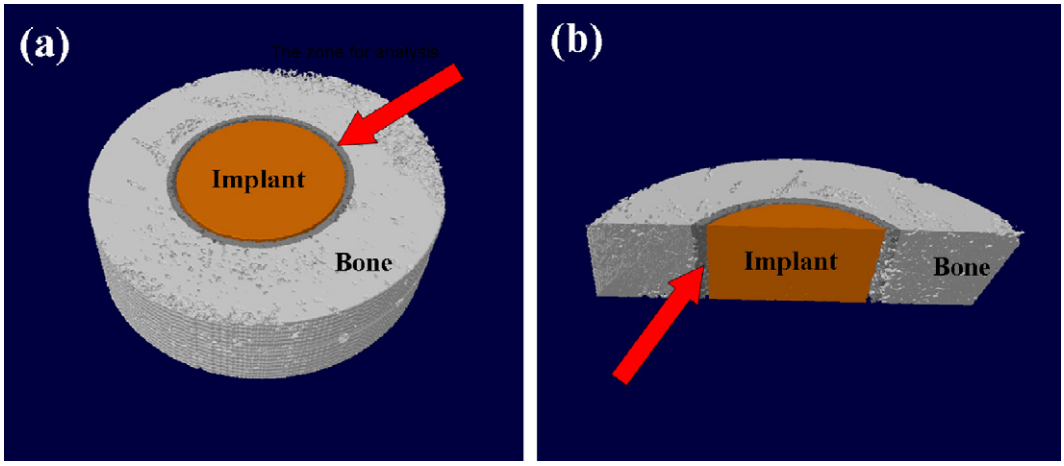

Fig. 2. 3D micro-CT reconstruction image of the mandible block containing one rod. (a) The top view; (b) the crossing-section view. The gray zone indicated by the arrow represented the zone of peri-rod for analysis.

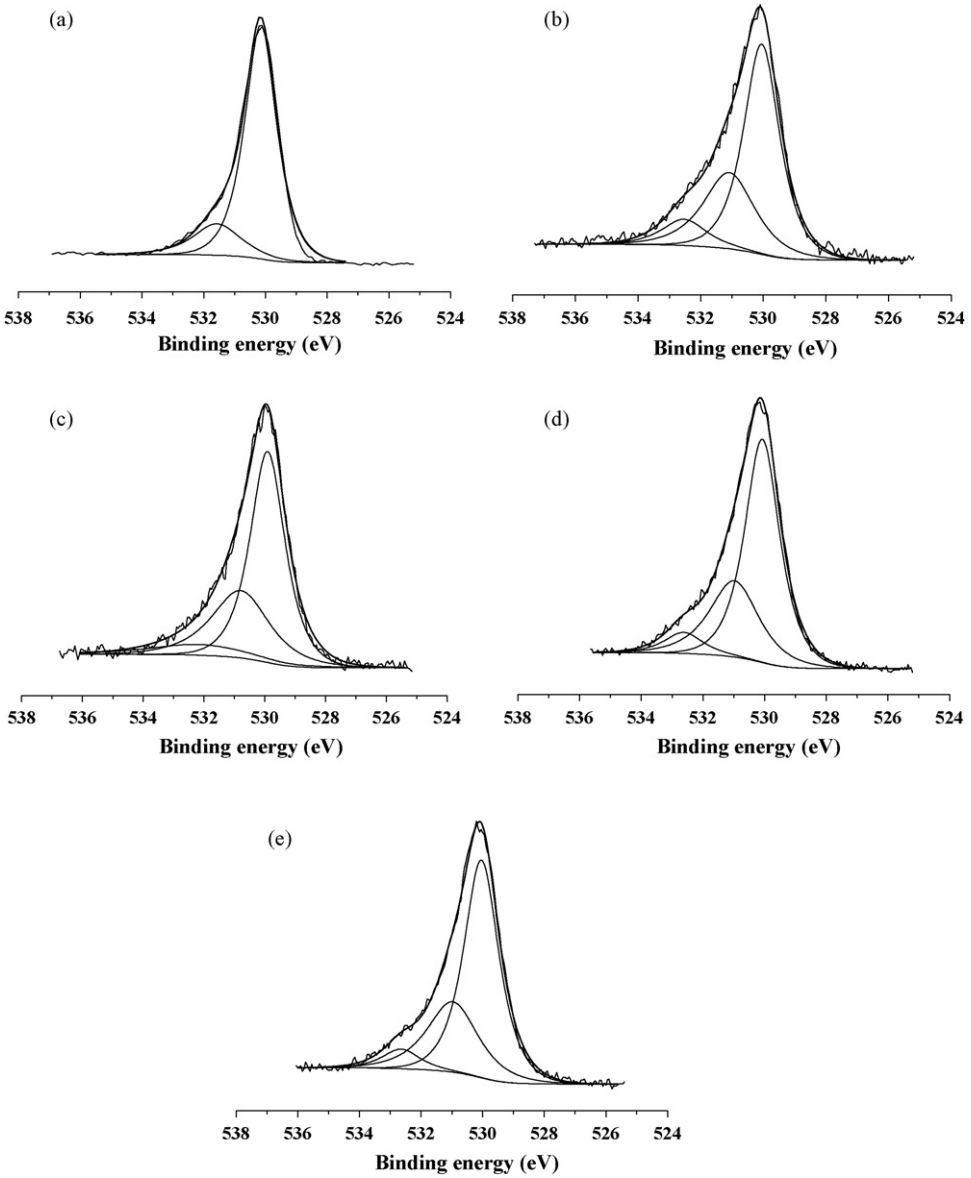

Fig. 3. High-resolution XPS spectra of O1s region of titanium disc before and after carbon dioxide plasma treatment. (a) Untreated; (b) treated at 20 W for 10 s; (c) treated at 20 W for 30 s; (d) treated at 20 W for 90 s; (e) treated at 20 W for 300 s.

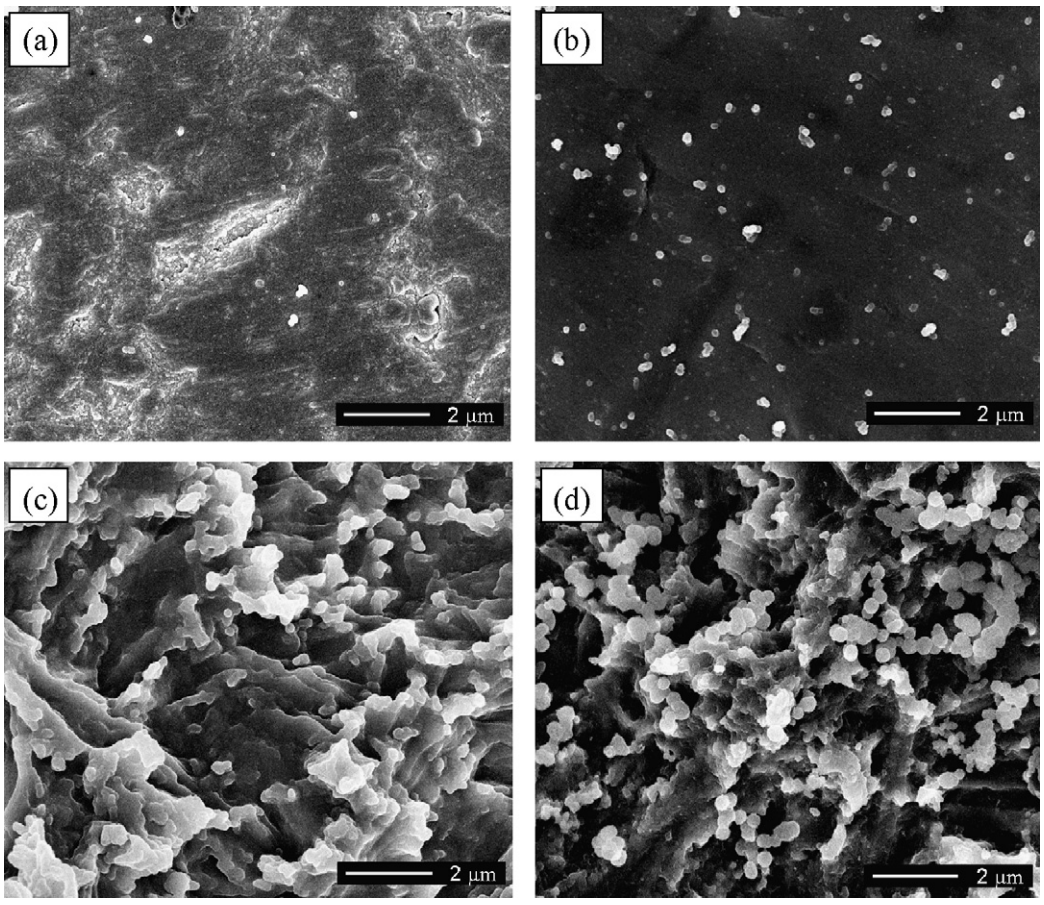

Fig. 4. Morphology observation of various titanium discs after incubation in 1.5SBF-2 for 3 days by SEM. (a) Untreated smooth titanium disc; (b) smooth titanium disc treated by carbon dioxide plasma under 20 W for 10 s; (c) sandblasted–acid etched titanium disc; (d) CPT-Ti disc.

culture medium was replaced with 1.5 ml of osteogenic media (α-MEM containing 10% fetal bovine serum, 100 U/cm^3 of penicillin, 100 U/cm^3 of streptomycin, 50 μg/mL of ascorbic acid, and 2 mM of β-glycerophosphate) per well. The osteogenic media were changed every 2 days. After the MC3T3-E1 cells were cultured on various titanium discs for 0, 3, 7, 10, 14 or 21 days in the osteogenic media, the discs were washed with PBS and 300 μl of 0.1% Triton X-100 was added to each well. After the MC3T3-E1 cells on the discs were frozen and then thawed repeatedly for 4 times, the solution was collected to measure the alkaline phosphatase (ALP) activity.

ALP activity was determined by using disodium phenyl phosphate as the substrate at pH 10. Each reaction was initiated with disodium phenyl phosphate, and allowed to proceed for 15 min at 37 °C, and then a developer potassium ferricyanide was quickly added. The absorbance at 520 nm was measured with UV spectrophotometer (752-type Ultraviolet grating spectrophotometer, Shanghai). The ALP activity was normalized by total intracellular protein synthesis and thus expressed as U/g protein. Total protein content was determined at 595 nm using a protein assay kit (Nanjing Jianchen Bioengineering Institute, China) according to manufacturer's instruction.

2.9. Animal test

All the experimental protocols were in compliance with the Animal Welfare Act and were approved by the Institutional Animal Care and Use Committee of Laboratory Animal Research Centre, at Chinese PLA General Hospital. Eighteen beagle dogs (age 12–15 months, mean weight 10.6 ± 1.2 kg) were used in the study. All dogs exhibited a fully erupted permanent dentition. During the experiment, the dogs were fed once per day with soft-food diet and water. The surgical site of the dogs under general anesthesia was disinfected with povidone iodine. The experimental samples were carefully implanted in the mandibles of the beagle dogs (Fig. 1). After implantation, the surgical incision was closed using Vicryl 5-0 sutures. The animals were divided into three groups of six, and observed after 4-, 8- and 12-week healing periods. All the dogs in each group were sacrificed by an intraperitoneal overdose injection of pentobarbital after 4, 8 and 12 weeks postoperation, respectively. Then the mandibles were explanted and fixed in 4% phosphate-buffered formalin solution.

2.10. Micro-computed tomography

After the animals were sacrificed, the mandibles including the rods were harvested. External soft tissue was removed and immediately fixed in 10% buffered formalin phosphate. The mandibles were divided into smaller specimens suitable for micro-CT scanning and histological processing. For a quantitative 3D analysis, the specimens were placed vertically onto the sample holder of a micro-CT imaging system, Skyscan 1076 desktop X-ray Micro-tomography System (SkyScan, Kontich, Belgium), with the long axis of the rod perpendicular to the scanning beam. Subsequently, each micro-CT image with gray color was acquired 15.5 min in which 600 views were obtained through 360° rotation using peak voltage 100 kV, current 80 μA. Then a cone beam reconstruction was performed on the projected files using Nrecon V1.6.0.3 (SkyScan, Kontich, Belgium). Finally, a 3D reconstruction of the rod and bone was obtained by using 3D creator software.

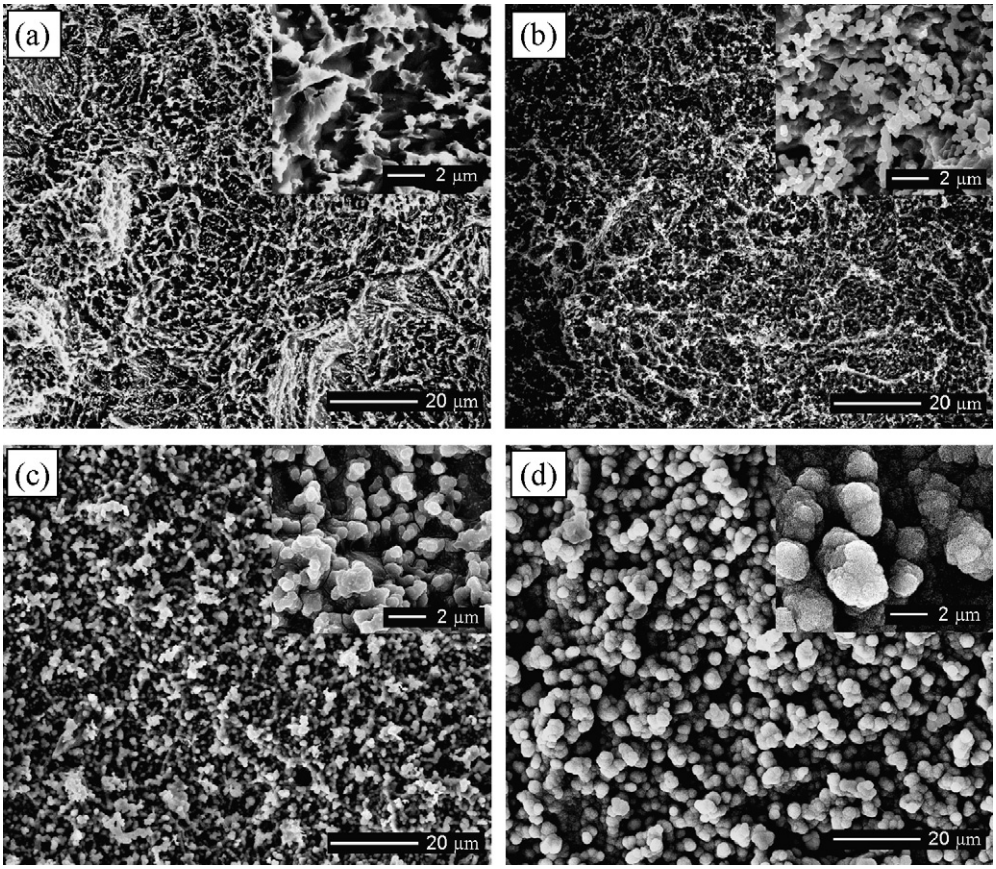

Fig. 5. The change of surface morphology of CPT-Ti discs incubated in 1.5SBF-2 with different times. (a) 0 day; (b) 3 days; (c) 7 days; (d) 14 days.

Prior to analysis, a constant region of interest (ROI) was set along the length of the rod, using CTAn, V1.9.2.5 (Skyscan, Kontich, Belgium). For all images annular ROI with the thickness of about 90 μm was manually selected to isolate bone tissue while excluding the rod materials (Fig. 2). Per rod, the parameters of bone mineral density (BMD), percentage of bone volume (BV/TV), trabecular thickness (Tb.Th.) and trabecular number (Tb.N.) were calculated.

2.11. Statistical analysis

Statistically significant differences ($p < 0.05$) between the various groups were measured using ANOVA and SNK post hoc. All statistical analyses were carried out using an SPSS 13.0 statistical software package. All the data are expressed as mean ± standard deviation (SD) ($n = 3$ or 4 for each group).

3. Results and discussion

3.1. Effect of carbon dioxide plasma treatment on hydrophilicity of titanium surface

After the titanium discs were treated by carbon dioxide plasma, surface hydrophilicity of the samples was immediately identified by measurements of contact angle to water. It was known from the result that the contact angles for smooth titanium discs and sandblasted–acid etched discs were 67.1° and 76.9°, respectively. After they were treated by carbon dioxide plasma under the power of 20 W, the contact angle of them quickly reduced 11.9° and <5°, respectively, which had no obvious difference with the treating time changed.

3.2. Effect of carbon dioxide plasma treatment on the chemistry of titanium surface

The chemical states of O before and after carbon dioxide plasma treatment were studied by XPS and the corresponding O1s spectra are shown in Fig. 3. The O1s peaks were resolved into three peaks with binding energies of 532.7, 531.4, and 530.2 eV, which could be attributed to the basic terminal hydroxyl groups associated with singly coordinated oxygen (532.7 eV), the acidic bridged hydroxyl groups associated with oxygen doubly coordinated with

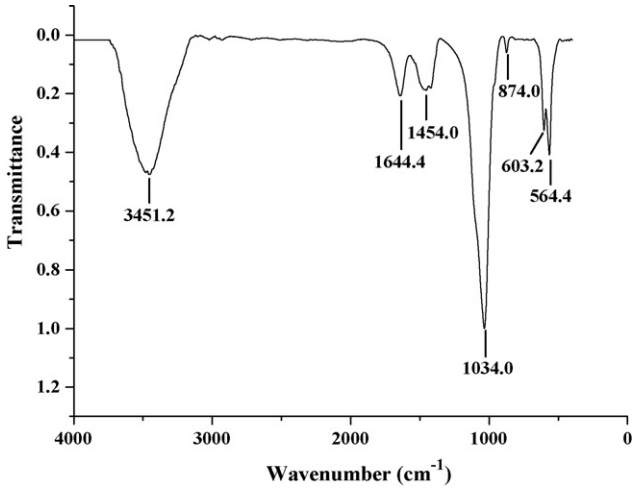

Fig. 6. FTIR spectrum of the hydroxyapatite powder obtained from CPT/SBF-Ti disc surface.

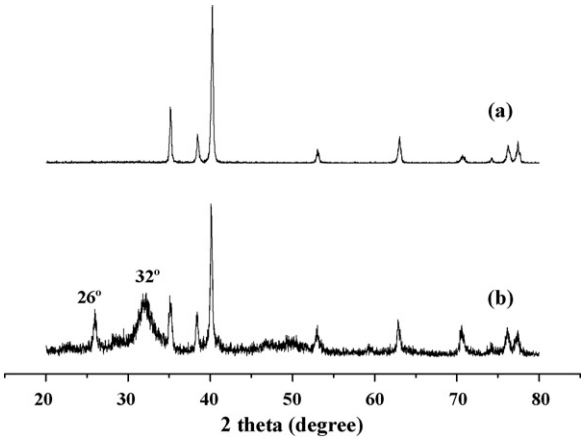

Fig. 7. XRD patterns of titanium disc. (a) CPT-Ti and (b) CPT/SBF-Ti.

titanium (531.4 eV), and O–Ti groups from TiO_2 (530.2 eV) [44–46], respectively (Fig. 3). The relative compositions of the three types of O1s changed with the time of carbon dioxide plasma treatment, as shown in Table 3. The fraction of basic terminal hydroxyl groups (basic OH) and acidic bridged hydroxyl groups (acidic OH) increased from 0% and 16.64% to 9.20% and 30.75% with the treating time increasing from 0 to 10 s, respectively. When the treating time reached to 30 s, basic OH and acidic OH changed to 8.29% and 31.57%, the sum of which was almost equal to that of the sample treated for 10 s. While with the treating time increasing to 90 and 300 s, the fraction of basic OH became 6.48% and 6.10%, and that of acidic OH decreased to 30.18% and 29.86%, respectively. It was concluded from the result that the basic OH and acidic OH on the surface of titanium discs were richest when the treatment time was controlled in 30 s. Therefore, we chose 10 s of treating time under 20 W as the treating parameters in this research. The sandblasted–acid etched titanium disc and rod treated for 10 s with carbon dioxide plasma under 20 W were abbreviated as CPT-Ti disc and rod.

The formation of the hydroxyl group could be explained that Ti–O bonds from the oxidized titanium and Ti–Ti bonds are easily destroyed by plasma treatment [47] and react with high energy reactive species generated by CO_2 plasma to produce hydroxyl groups.

3.3. Choice of 1.5SBF incubation solution

Because the growth rate of hydroxyapatite layer increased with increasing the ion concentration of SBF [48], two kinds of modified 1.5SBF were prepared as the incubation solution (Tables 1 and 2) in the present research. The CPT-Ti discs were incubated in 1.5SBF-1 and 1.5SBF-2 for 7 days to form hydroxyapatite coatings and determined the ratio of Ca/P by EDS. The quantitative analysis by the standardless mode gave Ca/P ratios of 1.34 and 1.64 for the hydroxyapatite layers formed in SBF-1 and SBF-2, respectively. The Ca/P ratio of the formed hydroxyapatite layer on the surface of titanium disc incubated in 1.5SBF-2 was almost equal with that of natural bone (1.67), so we chose 1.5SBF-2 as the incubating solution in this study.

3.4. Effect of sandblasting–acid-etching and carbon dioxide plasma treatment on the formation of hydroxyapatite

After incubation in 1.5SBF-2 for 3 days, surface morphologies of untreated smooth titanium discs, smooth titanium discs treated with carbon dioxide plasma under 20 W for 10 s, sandblasted–acid etched titanium discs and CPT-Ti discs were observed by SEM, as

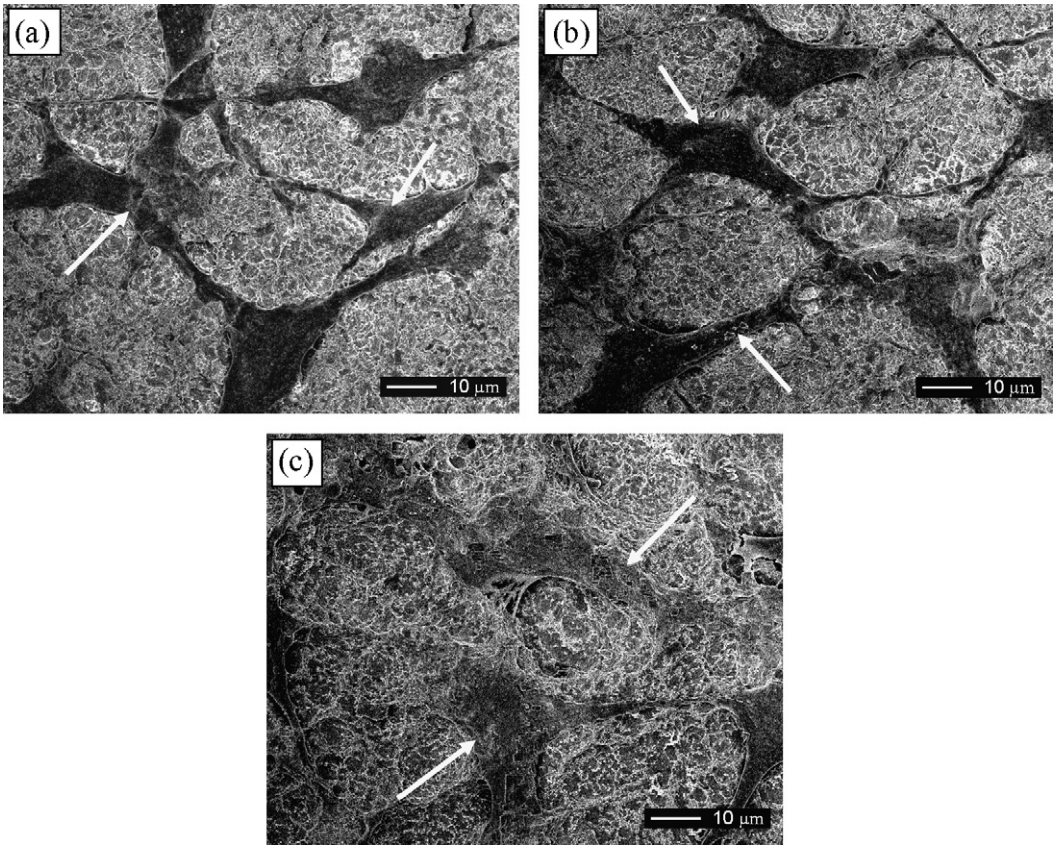

Fig. 8. Scanning electron micrographs of MC3T3-E1 cells cultured on various titanium discs for 4 h. (a) Ti; (b) CPT-Ti; (c) CPT/SBF-Ti, where the arrows indicate cells.

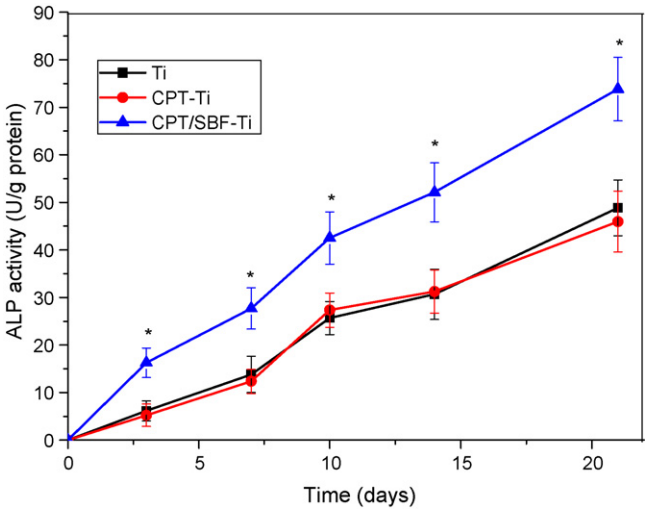

Fig. 9. ALP activity of MC3T3-E1 cells cultured on various titanium discs within different periods. ALP activity was determined as the enzyme activity unit (U) per gram of protein. $^{*}p < 0.05$: significant against ALP activity of MC3T3-E1 cells on Ti and CPT-Ti discs at the corresponding day.

shown in Fig. 4. There were a few of scattered particles on the surface of untreated smooth titanium discs (Fig. 4a). After carbon dioxide plasma treatment, the formed particles increased obviously (Fig. 4b). It meant that the amount of formed hydroxyapatite on the surface of titanium increased after it was modified with carbon dioxide plasma treatment under 20 W for 10 s. On the other hand, it could be seen from Fig. 4a and c that hydroxyapatite particles on the surface of sandblasted–acid etched disc were more than that on the untreated smooth titanium disc. In all of the samples, the hydroxyapatite particles formed on the surface of CPT-Ti disc were the most and largest (Fig. 4d).

From the results, two factors of the surface morphologies obtained by sandblasted-acid-etching and chemical groups introduced by carbon dioxide plasma treatment enhanced the hydroxyapatite formability of titanium surface when it was incubated in SBF. The reason for this was believed that the formation of basic OH and acidic OH on surface of titanium disc by carbon dioxide plasma treatment gave rise to hydroxyapatite precipitation because they could attract phosphate and calcium ions, respectively from the solution, which was the most crucial step to initiate the growth of the hydroxyapatite on the surface of biocompatible implants [45,49]. What's more, surface micro- and nano-structured topography produced by sandblasting–acid-etching method might increase the number of hydroxyapatite nucleation site, which enhanced the hydroxyapatite formation rate.

3.5. *Effect of incubating time on surface morphologies of CPT-Ti disc incubated in 1.5SBF-2*

The change of surface morphologies of CPT-Ti discs incubated in 1.5SBF-2 with different incubating time was observed by SEM,

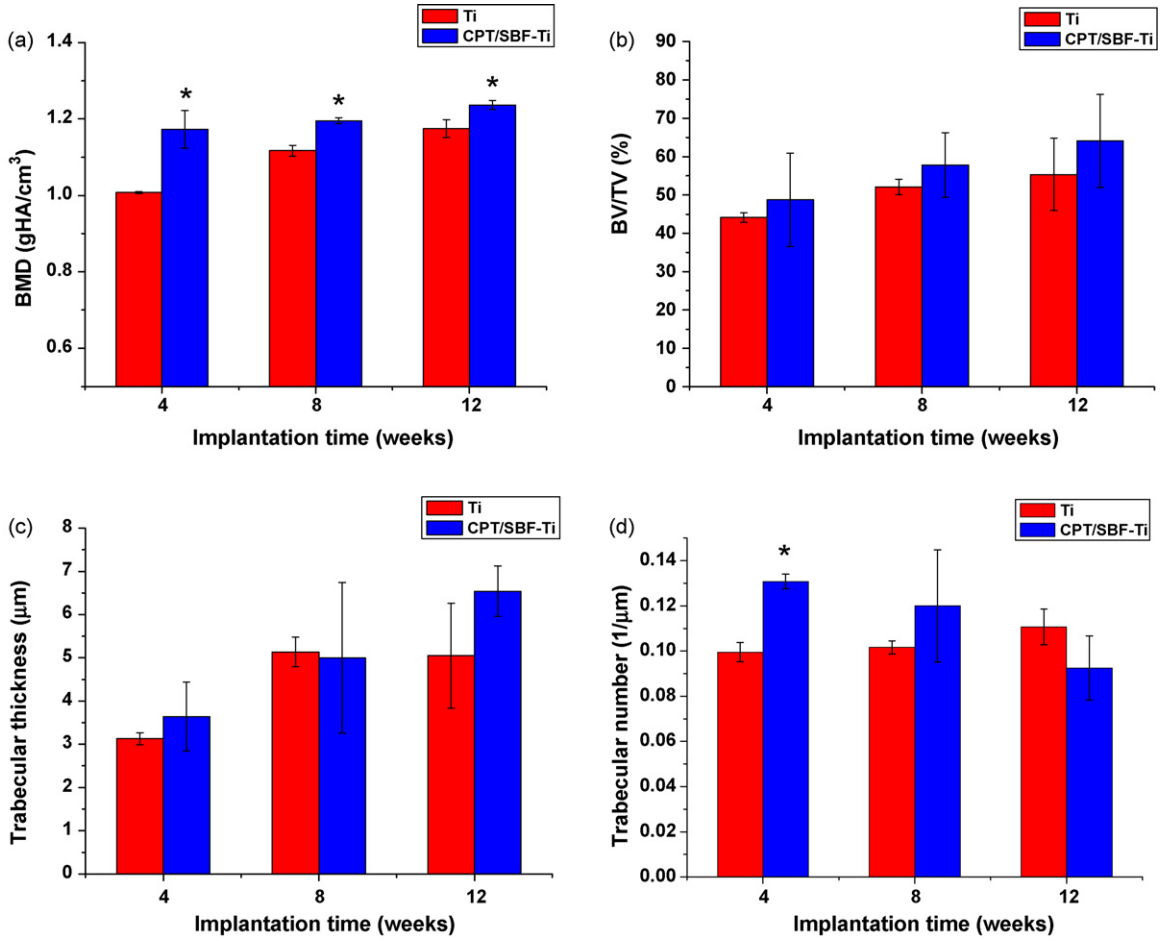

Fig. 10. Effect of surface modification on bone parameters of peri-rod after 4-, 8- and 12-week implantation periods, respectively. (a) Local bone mineral density (BMD) analysis; (b) a ratio of bone volume to total volume (BV/TV); (c) trabecular thickness (Tb.Th.); (d) trabecular number (Tb.N.). $^{*}p < 0.05$: significant against the parameters around Ti rods at the corresponding day.

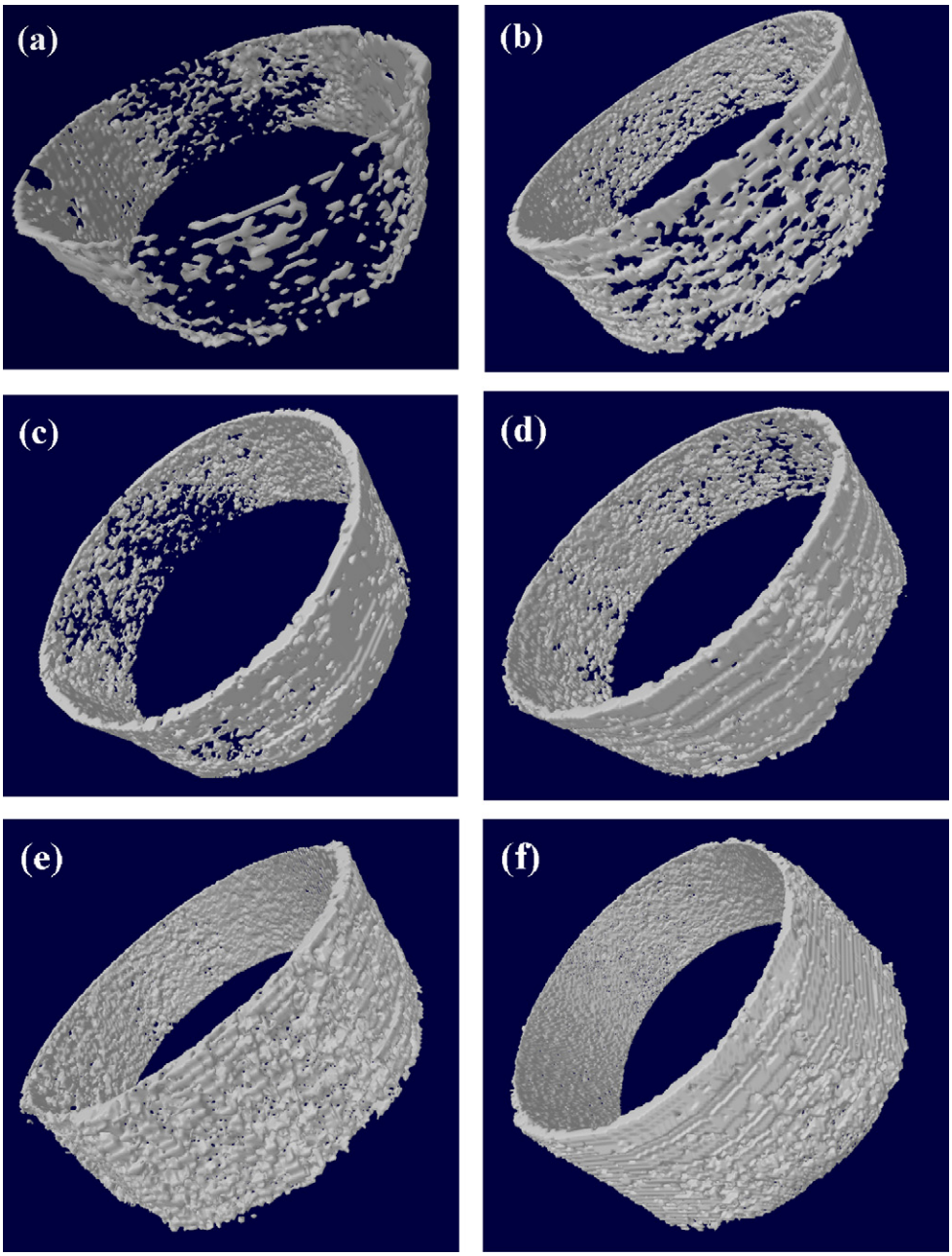

Fig. 11. 3D structure of the newly formed bone around the CPT/SBF-Ti and Ti rods reconstructed by micro-computed tomography (micro-CT) at various postoperative time-points. (a) Ti for 4 weeks; (b) CPT/SBF-Ti for 4 weeks; (c) Ti for 8 weeks; (d) CPT/SBF-Ti for 8 weeks; (e) Ti for 12 weeks; (f) CPT/SBF-Ti for 12 weeks.

as shown in Fig. 5. It could be seen from Fig. 5a that on the surface of the CPT-Ti disc many holes with the size of about 15–30 μm were produced by sandblasting. At the same time, more micro- and nano-dots (0.4–2 μm) developed by the acid-etching treatment were observed under high magnification on the surface. When the CPT-Ti disc was incubated in 1.5SBF-2 for 3 days at 36.5 °C, there were many hydroxyapatite particles on the surface, the particle size of which was about 350 nm, and the bare surface still could be seen (Fig. 5b). With the incubating time increasing to 7 days, more particles were formed on the surface of titanium, and the diameter of the particles was as big as about 600 nm, as shown in Fig. 5c. When the incubating time was further prolonged to 14 days, hydroxyapatite particles grew to about 2 μm, which completely covered the surface of the titanium disc (Fig. 5d). It was known from the above result that the size and quantity of hydroxyapatite particles increased with the incubation time increasing. Here, the CPT-Ti disc and rod incubated in 1.5SBF-2 for 7 days were abbreviated as CPT/SBF-Ti disc and rod.

3.6. FTIR and XRD characterization of hydroxyapatite on CPT/SBF-Ti disc

The chemical structure of the newly formed particles was examined by FTIR and XRD spectroscopy after the CPT-Ti disc was incubated in 1.5SBF-2 for 7 days, as shown in Figs. 6 and 7. Fig. 6 shows typical characteristics of the hydroxyapatite phase. The P=O stretching mode presents at ~1034.0 cm^{-1}. The absence of the peaks of P–O bending mode at ~564.4 and ~603.2 cm^{-1} indicates that this is an amorphous phosphate [50]. The peak at 874.0 cm^{-1} is due to the joint contribution of the carbonate and HPO_4^{2-} ions. A broad band at 1454.0 results from CO_3^{2-} group. An intensive broad band at 2500–3700 cm^{-1} originates from the asymmetrical

and symmetrical stretching vibrations of the O–H groups. The peak at 1644.4 cm^{-1} attributes to O–H of water absorbed in the sample. Overall, the spectrum indicated that the newly formed layer was an amorphous hydroxyapatite.

XRD analysis results of titanium disc before and after immersion in 1.5SBF-2 are shown in Fig. 7. After 7 days of incubation in 1.5SBF-2 the broad peaks at $2\theta = 26^\circ$ and $2\theta = 32^\circ$ generated by hydroxyapatite were observed, which suggested the amorphous compound was formed on the surface of titanium disc.

From above results, it was well known that the newly formed hydroxyapatite on surface of the titanium disc was an amorphous structure, which had a composition and structure analogous to those in bones [51].

3.7. Effect of the modified titanium on cell behavior

In order to examine cell responses to the modified titanium, the morphology and differentiation of the cell on the CPT/SBF-Ti disc were identified and compared with that on the sandblasted–acid etched titanium (Ti) discs and CPT-Ti discs using MC3T3-E1 cell as a model cell.

Fig. 8 shows morphology of MC3T3-E1 cells on various titanium discs after cultured for 4 h. It could be seen that after being cultured for 4 h, the cells on all of titanium discs could spread well and exhibit many filopodia (Fig. 8a–c). However, the morphology of cells on CPT/SBF-Ti discs was different from that on the Ti and CPT-Ti discs. The MC3T3-E1 cells on the Ti and CPT-Ti discs showed an elongated form (Fig. 8a and b), but most of cells on the CPT/SBF-Ti were flattened, showing polygonal shape, and the cellular filopodia more tightly anchored to the substrate (Fig. 8c).

The differentiated function of MC3T3-E1 cells on various titanium discs was evaluated by monitoring ALP activity of the cells. ALP is a marker enzyme of cells and probably involves in mineralization process. As shown in Fig. 9, the activity of ALP had a significant increase within 21 days on all of the titanium. The cells on the Ti and CPT-Ti discs exhibited the same ALP activity. However, the cells on the CPT/SBF-Ti disc showed much higher ALP activity than that on the Ti and CPT-Ti. The results showed that the ALP activity of MC3T3-E1 cells on the CPT/SBF-Ti was enhanced.

Connecting results of cell morphology observation and cell differentiation revealed that the carbon dioxide plasma treatment have no obvious effect on the MC3T3-E1 cell grow and differentiation. It was the formed nano-size hydroxyapatite that enhanced MC3T3-E1 cell adhesion and differentiation towards osteoblasts. Therefore, the carbon dioxide plasma treatment and then incubated in 1.5SBF-2 was expected to be an excellent method for the fabrication of titanium implant with good bioactivity and osteoconductivity.

3.8. Micro-CT analysis

Because the results of cell culture in vitro (Section 3.7) indicated plasma treatment had no obvious effect on modifying bioactivity of titanium, only the Ti and CPT/SBF-Ti rods were investigated in vivo. The parameters of the new bone tissue around the rods were automatically measured by micro-CT scan, as shown in Fig. 10. From the results, it was known that higher bone mineral density (BMD) was achieved around the CPT/SBF-Ti rod comparing with the control group of Ti. The value increased with implantation time increasing and BMD of peri-rods demonstrated the highest value of 1.236 g HA/cm^3 after a 12-week implantation period. Regarding bone mineral density there was a significant difference between the control rod of Ti and the modified implant of CPT/SBF-Ti ($p < 0.05$) (Fig. 10a). It was obvious that CPT/SBF-Ti improved the new bone formation of peri-rods compared to the control sample of Ti. At 12 weeks postoperative CPT/SBF-Ti increased significantly in BV/TV compared to the 4- and 8-week healing periods. For the CPT/SBF-Ti the value of the median percentage of bone volume (BV/TV) was 64.11% and that of the Ti was 55.35% at 12-week implantation period (Fig. 10b), but their difference was not significant.

Trabecular characteristics at different postoperative time-points are depicted in Fig. 10c and d. It could be seen from the results that the trabecular thickness (Tb.Th.) rose significantly for CPT/SBF-Ti from 4 to 12 weeks, but the Tb.Th. had no significant difference between the CPT/SBF-Ti and the Ti at all time-points. Trabecular number (Tb.N.) increased with implantation time increasing for the Ti and decreased for the CPT/SBF-Ti. For the CPT/SBF-Ti and Ti the Tb.N. were 0.134 and 0.105 μm^{-1} after 4-week implantation, respectively, and there was a significant difference. After a 12-week healing period the Tb.N. of the CPT/SBF-Ti and the Ti reached to 0.0924 and 0.111 μm^{-1}, respectively, which showed no significant difference. The results indicated that the HA coating obviously promoted bone formation during 4 weeks postoperative.

The morphology of the newly formed bone around the CPT/SBF-Ti and Ti rods was reconstructed using micro-CT at various postoperative time-points, as shown in Fig. 11. It was could be seen that for the CPT/SBF-Ti and Ti rods more new bone was formed with implantation time increasing in the annular region between the rod and natural bone, and there was less newly formed bone around the Ti rod than that round the CPT/SBF-Ti at the same postoperative time. Many single newly formed trabecular bones were scattered in the annular region for the Ti rods (Fig. 11a) and net-like bone was visible in the region for the CPT/SBF-Ti (Fig. 11b) 4 weeks postoperation. With the implantation time increasing more trabecular bone was formed and connected with each other (Fig. 11c and d). The annular loose bone structure with many pores was obtained around the Ti rod (Fig. 11e) when compared to the dense bone structure around the CPT/SBF-Ti (Fig. 11f) after 12-week implantation period.

It could be concluded from the above results that Ti modified by carbon dioxide plasma treatment and then incubated in SBF improved new bone formation of peri-rod, which consisted with that of cell culture in vitro.

4. Conclusions

In this study, sandblasted–acid etched titanium discs and rods were treated by carbon dioxide plasma and then incubated in a modified simulated body fluid to prepare a hydroxyapatite layer. It was found that the hydrophilicity of titanium sample was improved and hydroxyl groups on the titanium surface increased after carbon dioxide plasma treatment. The hydroxyapatite formability on the surface of sandblasted–acid etched titanium was enhanced by carbon dioxide plasma pretreatment. The reason for this was that carbon dioxide plasma treatment could increase negative charge of the titanium surface, which is effective on inducing hydroxyapatite nucleation. The morphology and differentiation of the cells cultured on Ti and CPT-Ti and CPT/SBF-Ti discs in vitro showed that the formed hydroxyapatite on CPT-Ti discs improved the attachment of MC3T3-E1 cells and stimulated the differentiation of them. On the other hand, the results of BMD, BV/TV, Tb.Th. and Tb.N. around the Ti and CPT/SBF-Ti rods, which were analyzed by the micro-CT after 4, 8 and 12 weeks implantation in vivo, indicated CPT/SBF-Ti enhanced new bone formation. Thus the method of carbon dioxide plasma treatment and then incubation in modified SBF could be a promising way to modify the titanium implants.

Acknowledgements

This research was supported by the State Key Development Program for Basic Research of China (Grant 2007CB936103), Peking University Interdisciplinary and Emerging Disciplines Research

Foundation (Grant PKUJC2009001), China Postdoctoral Science Foundation (20090450242), and Peking University's 985 Grant.

References

[1] D.M. Brunette, P. Tengvall, M. Textor, P. Thomsen, Titanium in Medicine, Springer, Berlin, 2001.
[2] R. Schenk, The corrosion properties of titanium and titanium alloys, in: B.D. Maxwell, P. Tengvall, M. Textor, P. Thomsen (Eds.), Titanium in Medicine, Berlin & Heidelberg, Springer, 2001, pp. 145–170.
[3] D. Steenberghe, R. Facobs, M. Desnyder, G. Maffei, M. Quirynen, The relative impact of local and endogenous patient-related factors on implant failure up to the abutment stage, Clin. Oral Implants Res. 13 (2002) 617–622.
[4] M. Petra, J. Diaz, P. Mclardy-Smith, D. Murray, R. Gundle, N.A. Athanasou, A correlative study of clinical and histological findings of revision hip arthroplasty for rheumatoid arthritis and inflammatory joint disease, Scand. J. Rheumatol. 32 (2003) 281–286.
[5] S.P. Johnsen, H.T. Sorensen, U. Lucht, K. Soballe, S. Overgaard, A.B. Pedersen, Patient-related predictors of implant failure after primary total hip replacement in the initial, short- and long-terms, J. Bone Joint Surg. Br. 88B (2006) 1303–1308.
[6] J.E. Davies (Ed.), The Bone–Biomaterial Interface, Univ Toronto, Toronto, 1991.
[7] D.A. Puleo, A. Nanci, Understanding and controlling the bone–implant interface, Biomaterials 20 (1999) 2311–2321.
[8] B. Elmengaard, J.E. Bechtold, K. Soballe, In vivo study of the effect of RGD treatment on bone ongrowth on press-fit titanium alloy implants, Biomaterials 26 (2005) 3521–3526.
[9] V. Borsari, M. Fini, G. Giavaresi, L. Rimondini, R. Chiesa, L. Chiusoli, et al., Sand-blasted titanium osteointegration in young, aged and ovariectomized sheep, Int. J. Artif. Organs 30 (2007) 163–172.
[10] W.Q. Yan, T. Nakamura, K. Kawanabe, S. Nishigochi, M. Oka, T. Kokubo, Apatite layer-coated titanium for use as bone bonding implants, Biomaterials 18 (1997) 1185–1190.
[11] H. Kim, S.H. Choi, J.J. Ryu, S.Y. Koh, J.H. Park, I.S. Lee, The biocompatibility of SLA-treated titanium implants, Biomed. Mater. 3 (2008) 25011–25016.
[12] S. Nishiguchi, T. Nakamura, M. Kobayashi, H.M. Kim, F. Miyaji, T. Kokubo, The effect of heat treatment on bone-bonding ability of alkali-treated titanium, Biomaterials 20 (1999) 491–500.
[13] K. Gotfredsen, E. Hjorting-Hansen, E. Budtz-Jörgensen, Clinical and radiographic evaluation of submerged and nonsubmerged implants in monkeys, Int. J. Prosthodont. 3 (1990) 463–469.
[14] D. Buser, N. Broggini, M. Wieland, R.K. Schenk, A.J. Denzer, D.L. Cochran, et al., Enhanced bone apposition to a chemically modified SLA titanium surface, J. Dent. Res. 83 (2004) 529–533.
[15] T. Kokubo, H.M. Kim, S. Nishiguchi, T. Nakamura, In vivo apatite formation induced on titanium metal and its alloys by chemical treatment, Key Eng. Mater. 192-1 (2000) 3–6.
[16] H.M. Kim, F. Miyaji, T. Kokubo, T. Nakamura, Preparation of bioactive Ti and its alloys via simple chemical surface treatment, J. Biomed. Mater. Res. 32 (1996) 409–417.
[17] M. Morra, C. Cassinelli, G. Cascardo, M. Fini, G. Giavaresi, R. Giardino, Covalently-linked hyaluronan promotes bone formation around Ti implants in a rabbit model, J. Orthop. Res. 27 (2009) 657–663.
[18] M. Morra, C. Cassinelli, G. Cascardo, P. Cahalan, L. Cahalan, M. Fini, et al., Surface engineering of titanium by collagen immobilization. Surface characterization and in vitro and in vivo studies, Biomaterials 24 (2003) 4639–4654.
[19] U. Fischer, U. Hempel, D. Becker, S. Bierbaum, D. Scharnweber, H. Worch, et al., Transforming growth factor beta 1 immobilized adsorptively on Ti6Al4V and collagen type I coated Ti6Al4V maintains its biological activity, Biomaterials 24 (2003) 2631–2641.
[20] K. Kashiwagi, T. Tsuji, K. Shiba, Directional BMP-2 for functionalization of titanium surfaces, Biomaterials 30 (2009) 1166–1175.
[21] T. Hanawa, Y. kamiura, S. Yamamoto, T. Kohgo, A. Amemiya, H. Ukai, et al., Early bone formation around calcium-ion-implanted titanium inserted into rat tibia, J. Biomed. Mater. Res. 36 (1997) 131–136.
[22] D. Krupa, J. Baszkiewicz, J.A. Kozubowski, A. Barcz, J.W. Sobczak, A. Biliński, et al., Effect of dual ion implantation of calcium and phosphorus on the properties of titanium, Biomaterials 26 (2005) 2847–2856.
[23] L.F. Cooper, Y.S. Zhou, J. Takebe, J.L. Guo, A. Abron, A. Holmen, et al., Fluoride modification effects on osteoblast behavior and bone formation at TiO_2 grit-blasted c.p. titanium endosseous implants, Biomaterials 27 (2006) 926–936.
[24] C. Wen, S. Guan, L. Peng, C. Ren, X. Wang, Z. Hu, Characterization and degradation behavior of AZ31 alloy surface modified by bone-like hydroxyapatite for implant applications, Appl. Surf. Sci. 255 (2009) 6433–6438.
[25] H.W. Denissen, K. Groot, P.C. Makkes, A. Hoff, P.J. Klopper, Tissue-response to dense apatite implants in rats, J. Biomed. Mater. Res. 14 (1980) 713–721.
[26] K.D. Groot, R. Geesink, C.P.A.T. Klein, P. Serekian, Plasma sprayed coatings of hydroxylapatite, J. Biomed. Mater. Res. 21 (1987) 1375–1381.
[27] R.L. Franco, R. Chiesa, M.M. Belot, P.T. Oliveira, A.L. Rosa, Human osteoblastic cell response to a Ca- and P-enriched titanium surface obtained by anodization, J. Biomed. Mater. Res. 88A (2009) 841–848.
[28] M. Ogiso, Y. Yamashita, T. Matsumoto, The process of physical weakening and dissolution of the HA-coated implant in bone and soft tissue, J. Dent. Res. 77 (1998) 1426–1434.
[29] J. Yang, J.Z. Bei, S.G. Wang, Enhanced cell affinity of Poly (D, L-lactide) by combing plasma treatment with collagen anchorage, Biomaterials 23 (2002) 2607–2614.
[30] W.L. Wade, R.J. Mammone, M. Binder, Surface-properties of commercial polymer-films following various gas plasma treatments, J. Appl. Polym. Sci. 43 (1991) 1589–1591.
[31] Y.X. Qiu, D. Klee, W. Pluster, B. Severich, H. Hocker, Surface modification of polyurethane by plasma-induced graft polymerization of poly(ethylene glycol) methacrylate, J. Appl. Polym. Sci. 61 (1996) 2373–2382.
[32] S.H. Hsu, W.C. Chen, Improved cell adhesion by plasma-induced grafting of L-lactide onto polyurethane surface, Biomaterials 21 (2000) 359–367.
[33] Y.Q. Wan, X. Qu, J. Lu, C.F. Zhu, L.J. Wan, J.L. Yang, et al., Characterization of surface property of poly(lactide-co-glycolide) after oxygen plasma treatment, Biomaterials 25 (2004) 4777–4783.
[34] X. Qu, W.J. Cui, F. Yang, C.C. Min, H. Shen, J.Z. Bei, et al., The effect of oxygen plasma pretreatment and incubation in modified simulated body fluids on the formation of bone-like apatite on poly(lactide-co-glycolide) (70/30), Biomaterials 28 (2007) 9–18.
[35] H. Shen, X.X. Hu, J.Z. Bei, S.G. Wang, The immobilization of basic fibroblast growth factor on plasma-treated poly(lactide-co-glycolide), Biomaterials 29 (2008) 2388–2399.
[36] P.K. Chu, J.Y. Chen, L.P. Wang, N. Huang, Plasma surface modification of biomaterials, Mater. Sci. Eng.: Rep. 36 (2002) 143–206.
[37] Y. Okabe, M. Iwaki, K. Takahashi, S. Ohira, B.V. Christ, Formation of rutile TiO_2 induced by high-dose O^+-implantation and its characteristics, Nucl. Instrum. Methods B 39 (1989) 619–622.
[38] Y. Okabe, T. Fujihana, M. Iwaki, B.V. Crist, Characterization of oxide layers induced by oxygen-ion implantation into Ti, V, Cr, Zr, Nb, Mo, Hf, Ta, and W, Surf. Coat. Technol. 66 (1994) 384–388.
[39] A. Loinza, M. Rinner, F. Alonso, J.I. Onate, W. Ensinger, Effects of plasma immersion ion implantation of oxygen on mechanical properties and microstructure of Ti6Al4V, Surf. Coat. Technol. 103–104 (1998) 262–267.
[40] Y.T. Xie, X.Y. Liu, A.P. Huang, C.X. Ding, P.K. Chu, Improvement of surface bioactivity on titanium by water and hydrogen plasma immersion ion implantation, Biomaterials 26 (2005) 6129–6135.
[41] J.G.A. Terlingen, H.F.C. Gerritsen, A.S. Hoffman, J. Feijen, J. Appl. Polym. Sci. 57 (1995) 969–982.
[42] H. Takadama, H.M. Kim, T. Kokubo, T. Nakamura, TEM-EDX study of mechanism of bonelike apatite formation on bioactive titanium metal in simulated body fluid, J. Biomed. Mater. Res. 57 (2001) 441–448.
[43] H. Takadama, H.M. Kim, T. Kokubo, T. Nakamura, An X-ray photoelectron spectroscopy study of the process of apatite formation on bioactive titanium metal, J. Biomed. Mater. Res. 55 (2001) 185–193.
[44] M.T. Pham, H. Reuther, W. Matz, R. Mueller, G. Steiner, S. Oswald, et al., Surface induced reactivity for titanium by ion implantation, J. Mater. Sci. Mater. Med. 11 (2000) 383–391.
[45] K.E. Healey, P. Ducheyne, Hydration and preferential molecular adsorption on titanium in vitro, Biomaterials 13 (1992) 553–561.
[46] M. Browne, P.J. Gregson, R.H. West, Characterization of titanium alloy implant surfaces with improved dissolution resistance, J. Mater. Sci. Mater. Med. 7 (1996) 323–329.
[47] Y. Choi, S. Yamamoto, H. Saitoh, T. Sumita, H. Itoh, Influence of carbon-ion irradiation and hydrogen-plasma treatment on photocatalytic properties of titanium dioxide films, Nucl. Instrum. Methods Phys. Res. Sect. B: Beam Interact. Mater. 206 (2003) 241–244.
[48] T. Kokubo, Formation of biologically active bone-like apatite on metals and polymers by a biomimetic process, Thermochim. Acta 280 (1996) 479–490.
[49] M. Svetina, L.C. Ciacchi, O. Sbaizero, S. Meriani, A.D. Vita, Deposition of calcium ions on rutile (110): a first-principles investigation, Acta Mater. 49 (2001) 2169–2177.
[50] M.R.T. Filgueiras, G. Latorre, L.L. Hench, Solution effects on the surface-reactions of three bioactive glass compositions, J. Biomed. Mater. Res. 27 (1993) 1485–1493.
[51] S.L. Turek, Physiology and mineralization of bone Orthopeadics: Principles & Their Applications, vol. 1, 4th ed., J.B. Lippincott Company, Philadelphia, 1984, pp. 136–144 (Chapter 6).